# TSB712A, TSB712

Datasheet

## Precision rail-to-rail input / output 36 V, 6 MHz dual op-amps

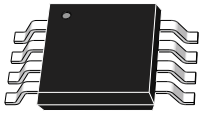

MiniSO8

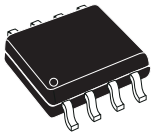

SO8

| Maturity status link |
|---|
| TSB712A, TSB712 |

| Related products | |
|---|---|
| TSB572 | Dual op-amps for the low-power consumption version (380 µA with 2.5 MHz GBP) |

## Features

- Rail-to-rail input and output
- Low offset voltage: 300 µV maximum
- Wide supply voltage range: 2.7 V to 36 V
- Gain bandwidth product: 6 MHz
- Slew rate : 3 V/µs
- Low noise : 12 nV/√Hz
- Integrated EMI filter
- Standard SO8 and miniSO8 packages
- 2 kV HBM ESD tolerance
- Extended temperature range : -40 °C to +125 °C
- Automotive-grade available

## Applications

- High-side and low-side current sensing
- Hall effect sensors
- Data acquisition and instrumentation
- Test and measurement equipments
- Motor control
- Industrial process control
- Strain gauge

## Description

The TSB712 and the TSB712A dual 6 MHz bandwidth amplifiers feature rail-to-rail input and output, which is guaranteed to operate from +2.7 V to +36 V single supply as well as from ±1.35 V to ±18 V dual supplies.

These amplifiers have the advantage of offering a large span of supply voltage and an excellent input offset voltage of 300 µV maximum at 25 °C.

The combination of wide bandwidth, slew rate, low noise, rail-to-rail capability and precision makes the TSB712 and the TSB712A useful in a wide variety of applications such as: filters, power supply and motor control, actuator driving, hall effect sensors and resistive transducers.

# 1 Pin description

Figure 2. **Pin connections (top view)**

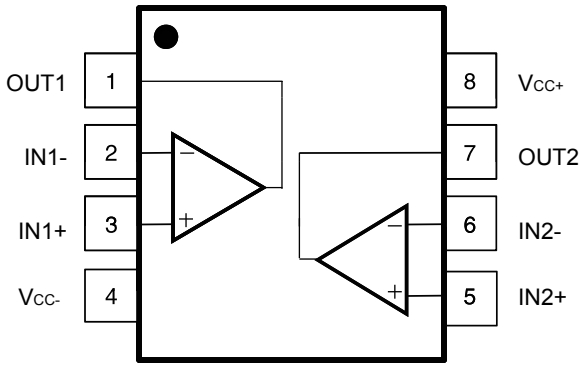


MiniSO8/SO8

| Pin | Pin name | Description |
|---|---|---|
| 1 | OUT1 | Output channel 1 |
| 2 | IN1- | Inverting input channel 1 |
| 3 | IN1+ | Non-inverting input channel 1 |
| 4 | $V_{CC-}$ | Negative supply voltage |
| 5 | IN2+ | Non-inverting input channel 2 |
| 6 | IN2- | Inverting input channel 2 |
| 7 | OUT2 | Output channel 2 |
| 8 | $V_{CC+}$ | Positive supply voltage |

# 2 Absolute maximum ratings and operating conditions

**Table 1. Absolute maximum ratings**

| Symbol | Parameter | Value | Unit |
|---|---|---|---|
| $V_{CC}$ | Supply voltage (1) | +40 or ±20 | V |
| $V_{id}$ | Input voltage differential (2) | ±2 | V |
| $V_{in}$ | Input voltage | ($V_{CC-}$) - 0.2 to ($V_{CC+}$) + 0.2 | V |
| $I_{in}$ | Input current (3) | ±10 | mA |
| | Storage temperature | -65 to +150 | °C |
| $R_{th-ja}$ | Thermal resistance junction-to-ambient (4) (5) | | °C / W |
| | MiniSO-8 | 190 | |
| $T_j$ | Maximum junction temperature | 150 | °C |
| ESD | HBM: human body model (6) | 2 | kV |
| | CDM: charged device model (7) | 1 | kV |
| | Latch-up immunity | 100 | mA |

1. *All voltage values, except the differential voltage are with respect to the network ground terminal.*
2. *Differential voltages are the non-inverting input terminal with respect to the inverting input terminal. The maximum input voltage differential value may be extended to the condition that the input current is limited to ±10 mA. See Section 5.2 Input pin voltage range.*
3. *Input current must be limited by a resistor in series with the inputs when the input voltage is beyond the rails (see Section 5.2 Input pin voltage range).*
4. *Short-circuits can cause excessive heating and destructive dissipation.*
5. *$R_{th}$ are typical values.*
6. *Human body according to JEDEC standard JESD22-A114F.*
7. *According to ANSI/ESD STM5.3.1.*

**Table 2. Operating conditions**

| Symbol | Parameter | Value |
|---|---|---|
| $V_{CC}$ | Supply voltage | 2.7 V to 36 V |
| $V_{icm}$ | Common mode input voltage range | ($V_{CC-}$) to ($V_{CC+}$) + 0.1 V |
| $T_{oper}$ | Operating free air temperature range | -40 °C to +125 °C |

# 3 Electrical characteristics

**Table 3. Electrical characteristics at $V_{CC}$ = 36 V, $V_{ICM}$ = $V_{OUT}$ = $V_{CC}$ / 2, $T_{amb}$ = 25 °C and $R_L$ connected to $V_{CC}$ / 2 (unless otherwise specified)**

| Symbol | Parameter | Conditions | Min. | Typ. | Max. | Unit |
|---|---|---|---|---|---|---|
| **DC performance** | | | | | | |
| $V_{io}$ | Input offset voltage | TSB712A, T = 25 °C, $V_{CC-} \le V_{ICM} \le V_{CC+}$ - 1.5 V | | | ± 300 | µV |
| | | TSB712A, T = 25 °C, $V_{CC-} \le V_{ICM} \le V_{CC+}$ | | | ± 650 | |
| | | TSB712A, -40 °C < T < 125 °C, $V_{CC-} \le V_{ICM} \le V_{CC+}$ - 1.5 V | | | ± 580 | |
| | | TSB712A, -40 °C < T < 125 °C, $V_{CC-} \le V_{ICM} \le V_{CC+}$ | | | ± 930 | |
| | | TSB712, T = 25 °C, $V_{CC-} \le V_{ICM} \le V_{CC+}$ -1.5 V | | | ± 800 | |
| | | TSB712, T = 25 °C, $V_{CC-} \le V_{ICM} \le V_{CC+}$ | | | ± 1200 | |
| | | TSB712, -40 °C < T < 125 °C, $V_{CC-} \le V_{ICM} \le V_{CC+}$ - 1.5 V | | | ± 1100 | |
| | | TSB712, -40 °C < T < 125 °C, $V_{CC-} \le V_{ICM} \le V_{CC+}$ | | | ± 1400 | |
| $\Delta V_{io}$ / $\Delta T$ | Input offset voltage drift | -40°C < T < 125 °C (1) | | | 2.8 | µV / °C |
| $\Delta V_{io}$ | Long-term input offset voltage drift | T = 25 °C (2) | | 0.57 | | µV / √mo |
| $I_{IB}$ | Input bias current (3) | $V_{ICM}$ = $V_{CC+}$, T = 25 °C | 0 | | 300 | nA |
| | | $V_{ICM}$ = $V_{CC+}$, -40 °C < T < 125 °C | 0 | | 900 | |
| | | $V_{ICM}$ = $V_{CC-}$, T = 25 °C | -100 | | 0 | |
| | | $V_{ICM}$ = $V_{CC-}$,-40 °C < T < 125 °C | -200 | | 0 | |
| $I_{IO}$ | Input offset current (4) | $V_{ICM}$ = $V_{CC+}$ | | 10 | | |
| | | $V_{ICM}$ = $V_{CC-}$ | | 10 | | |

| Symbol | Parameter | Conditions | Min. | Typ. | Max. | Unit |
|---|---|---|---|---|---|---|
| $A_{VD}$ | Open loop gain | $R_L \geq 10\ k\Omega$, $(V_{CC-}) + 0.5\ V \leq V_{OUT} \leq (V_{CC+}) - 0.5\ V$, T = 25 °C | 110 | 125 | | dB |
| | | $R_L \geq 10\ k\Omega$, $(V_{CC-}) + 0.5\ V \leq V_{OUT} \leq (V_{CC+}) - 0.5\ V$, -40 °C < T < 125 °C | 105 | | | |
| CMR | Common-mode rejection ratio 20 log ($\Delta V_{INCM}$ / $\Delta V_{IO}$) | $(V_{CC-}) \leq V_{ICM} \leq (V_{CC+}) - 1.5\ V$, T = 25 °C | 115 | 130 | | |
| | | $(V_{CC-}) \leq V_{ICM} \leq (V_{CC+}) - 1.5\ V$, -40 °C < T < 125 °C | 110 | | | |
| | | TSB712 A $(V_{CC-}) \leq V_{ICM} \leq (V_{CC+})$, T = 25 °C | 100 | 120 | | |
| | | TSB712 A $(V_{CC-}) \leq V_{ICM} \leq (V_{CC+})$, -40 °C < T < 125 °C | 95 | | | |
| | | TSB712 $(V_{CC-}) \leq V_{ICM} \leq (V_{CC+})$, T = 25 °C | 90 | 120 | | |
| | | TSB712 $(V_{CC-}) \leq V_{ICM} \leq (V_{CC+})$, -40 °C < T < 125 °C | 85 | | | |
| SVR | Power supply rejection ratio 20 log ($\Delta V_{CC}$ / $\Delta V_{IO}$) | $5\ V < (V_{CC+}) - (V_{CC-}) < 36\ V$, $V_{ICM} = V_{CC} / 2$ -40 °C < T < 125 °C | 100 | 125 | | |
| $V_{OH}$ | High level output voltage (drop voltage from $V_{CC+}$) | No load, -40 °C < T < 125 °C | | | 120 | mV |
| | | $I_{SOURCE}$ = 2 mA, -40 °C < T < 125 °C | | | 200 | |
| | | $I_{SOURCE}$ = 15 mA, -40 °C < T < 125 °C | | | 1000 | |
| $V_{OL}$ | Low level output voltage | No load , -40 °C < T < 125 °C | | | 120 | |
| | | $I_{SINK}$ = 2 mA, -40 °C < T < 125 °C | | | 200 | |
| | | $I_{SINK}$ = 15 mA , -40 °C < T < 125 °C | | | 1000 | |
| $I_{OUT}$ | $I_{SINK}$ | $V_{OUT} = V_{CC}$, T = 25 °C | 25 | 50 | | mA |
| | | $V_{OUT} = V_{CC}$, -40 °C < T < 125 °C | 20 | | | |
| | $I_{SOURCE}$ | $V_{OUT}$ = 0 V, T = 25 °C | 25 | 50 | | |
| | | $V_{OUT}$ = 0 V, -40 °C < T < 125 °C | 20 | | | |
| $I_{CC}$ | Supply current by op-amp | No load, T = 25 °C | | 1.8 | | mA |
| | | No load, -40 °C < T < 125 °C | | | 3 | |
| **AC performance** | | | | | | |
| GBP | Gain bandwidth product | $R_L$ = 10 kΩ, $C_L$ = 100 pF | 4.5 | 6 | | MHz |
| SR | Slew rate | 9 V step, $R_L$ = 10 kΩ, $C_L$ = 100 pF, $A_V$ = 1 V/V, 10% to 90% | 2.2 | 3 | | V / µs |
| THD+N | Total harmonic distorsion + noise | $V_{IN}$ = 1 Vrms , $R_L$ = 10 kΩ, $A_V$ = +1, f = 1 kHz, BW = 22 kHz | | 0,0003 | | % |
| | | $V_{IN}$ = 1 Vrms , $R_L$ = 1 kΩ, $A_V$ = +1, f = 1 kHz, BW = 22 kHz | | 0,00034 | | |

| Symbol | Parameter | Conditions | Min. | Typ. | Max. | Unit |
|---|---|---|---|---|---|---|
| CR | Crosstalk | $V_{OUT}$ = 5 Vpp, f = 1 kHz, $A_V$ = +11, $R_L$ = 10 kΩ | | 125 | | dB |
| | | $V_{OUT}$ = 5Vpp, f = 10 kHz, $A_V$ = +11, $R_L$ = 10 kΩ | | 100 | | |
| Φm | Phase margin | At unity gain, 25 °C, 10 kΩ, 100 pF | | 45 | | ° |
| $C_{LOAD}$ | Capacitive load drive | | | 100(5) | | pF |
| en | Input voltage noise density | f = 10 Hz | | 20 | | nV / √Hz |
| | | f = 100 Hz | | 13 | | |
| | | f = 10 kHz | | 12 | | |
| en p-p | Input noise voltage | 0.1 Hz ≤ f ≤ 10 Hz | | 0.5 | | $\mu V_{PP}$ |
| in | Input current noise density | f = 1 kHz | | 0.15 (6) | | pA / √Hz |

1. *See Section 5.4 Input offset voltage drift over the temperature in application information.*
2. *Typical value is based on the $V_{IO}$ drift observed after 1000 h at 125 °C extrapolated to 25 °C using the Arrhenius law and assuming an activation energy of 0.7 eV. The operational amplifier is aged in follower mode configuration. See Section 5.5 Long term input offset voltage drift.*
3. *Current is positive when it is sinked into the op-amp.*
4. *$I_{io}$ is defined as $|I_{ibp} – I_{ibn}|$*
5. *For higher capacitive values see Figure 25. Phase margin vs. output current at $V_{CC}$ = 36 V, Figure 26. Phase margin vs. capacitive load and Figure 27. Overshoot vs. capacitive load at $V_{CC}$ = 36 V*
6. *Theoretical value of the input current noise density based on the measurement of the input transistor base current: $i_n = \sqrt{2.q.i_b}$*

**Table 4. Electrical characteristics at $V_{CC}$ = 5 V, $V_{ICM}$ = $V_{OUT}$ = $V_{CC}$ / 2, $T_{amb}$ = 25 °C and $R_L$ connected to $V_{CC}$ / 2 (unless otherwise specified)**

| Symbol | Parameter | Conditions | Min. | Typ. | Max. | Unit |
|---|---|---|---|---|---|---|
| **DC performance** | | | | | | |
| $V_{io}$ | Input offset voltage | TSB712A, T = 25 °C, $V_{CC-} \le V_{ICM} \le V_{CC+}$ - 1.5 V | | | ± 350 | µV |
| | | TSB712A, T = 25 °C, $V_{CC-} \le V_{ICM} \le V_{CC+}$ | | | ± 650 | |
| | | TSB712A, -40 °C < T < 125 °C, $V_{CC-} \le V_{ICM} \le V_{CC+}$ - 1.5 V | | | ± 750 | |
| | | TSB712A, -40 °C < T < 125 °C, $V_{CC-} \le V_{ICM} \le V_{CC+}$ | | | ± 1050 | |
| | | TSB712, T = 25 °C, $V_{CC-} \le V_{ICM} \le V_{CC+}$ - 1.5 V | | | ± 800 | |
| | | TSB712, T = 25 °C, $V_{CC-} \le V_{ICM} \le V_{CC+}$ | | | ± 1200 | |
| | | TSB712, -40 °C < T < 125 °C, $V_{CC-} \le V_{ICM} \le V_{CC+}$ - 1.5 V | | | ± 1100 | |
| | | TSB712, -40 °C < T < 125 °C, $V_{CC-} \le V_{ICM} \le V_{CC+}$ | | | ± 1400 | |
| $\Delta V_{io}$ / $\Delta T$ | Input offset voltage drift | -40°C < T < 125 °C (1) | | | 4 | µV / °C |
| $I_{IB}$ | Input bias current (2) | $V_{ICM} = V_{CC+}$, T = 25 °C | 0 | | 300 | nA |
| | | $V_{ICM} = V_{CC+}$, -40 °C < T < 125 °C | 0 | | 900 | |
| | | $V_{ICM} = V_{CC-}$, T = 25 °C | -100 | | 0 | |
| | | $V_{ICM} = V_{CC-}$, -40 °C < T < 125 °C | -200 | | 0 | |
| $I_{IO}$ | Input offset current (3) | $V_{ICM} = V_{CC+}$ | | 10 | | |
| | | $V_{ICM} = V_{CC-}$ | | 10 | | |
| $A_{VD}$ | Open loop gain | $R_L \ge 10$ kΩ, $(V_{CC-}) + 0.5\ V \le V_{OUT} \le (V_{CC+}) - 0.5\ V$, T = 25 °C | 105 | 120 | | dB |
| | | $R_L \ge 10$ kΩ, $(V_{CC-}) + 0.5\ V \le V_{OUT} \le (V_{CC+}) - 0.5\ V$, -40 °C < T < 125 °C | 100 | | | |

| Symbol | Parameter | Conditions | Min. | Typ. | Max. | Unit |
|---|---|---|---|---|---|---|
| CMR | Common-mode rejection ratio<br>20 log ( $\Delta V_{INCM}$ / $\Delta V_{IO}$ ) | ($V_{CC-}$) ≤ $V_{ICM}$ ≤ ( $V_{CC+}$) - 1.5 V,<br>T = 25 °C | 95 | 125 | | dB |
| | | ($V_{CC-}$) ≤ $V_{ICM}$ ≤ ($V_{CC+}$) - 1.5 V,<br>-40 °C < T < 125 °C | 90 | | | |
| | | TSB712A ($V_{CC-}$) ≤ $V_{ICM}$ ≤ ($V_{CC+}$),<br>T = 25 °C | 80 | 105 | | |
| | | TSB712A ($V_{CC-}$) ≤ $V_{ICM}$ ≤ ($V_{CC+}$),<br>-40 °C < T < 125 °C | 75 | | | |
| | | TSB712 ($V_{CC-}$) ≤ $V_{ICM}$ ≤ ($V_{CC+}$),<br>T = 25 °C | 75 | 105 | | |
| | | TSB712 ($V_{CC-}$) ≤ $V_{ICM}$ ≤ ($V_{CC+}$),<br>-40 °C < T < 125 °C | 70 | | | |
| $V_{OL}$ | Voltage output swing from positive rail<br>($V_{CC+}$) - ($V_{OH}$) | No load, -40 °C < T < 125 °C | | | 90 | mV |
| | | $I_{SOURCE}$ = 2 mA, -40 °C < T < 125 °C | | | 200 | |
| $V_{OH}$ | Voltage output swing from negative rail<br>($V_{OL}$) - ($V_{CC-}$) | No load, -40 °C < T < 125 °C | | | 90 | |
| | | $I_{SINK}$ = 2 mA, -40 °C < T < 125 °C | | | 200 | |
| $I_{OUT}$ | $I_{SINK}$ | $V_{OUT}$ = $V_{CC}$, T = 25 °C | 20 | 50 | | mA |
| | | $V_{OUT}$ = $V_{CC}$, -40 °C < T < 125 °C | 15 | | | |
| | $I_{SOURCE}$ | $V_{OUT}$ = 0 V, T = 25 °C | 20 | 50 | | |
| | | $V_{OUT}$ = 0 V, -40 °C < T < 125 °C | 15 | | | |
| $I_{CC}$ | Supply current by op-amp | No load, T = 25 °C | | 1.4 | | mA |
| | | No load, -40 °C < T < 125 °C | | | 2.3 | |
| **AC performance** | | | | | | |
| GBP | Gain bandwidth product | $R_L$ = 10 kΩ, $C_L$ = 100 pF | 4.5 | 6 | | MHz |
| SR | Slew rate | 3 V step, $R_L$ = 10 kΩ, $C_L$ = 100 pF,<br>$A_V$ = 1 V/V, 10% to 90% | 2 | 2.7 | | V / µs |
| THD+N | Total harmonic distorsion + noise | $V_{IN}$ = 1 Vrms , $R_L$ = 10 kΩ, $A_V$ = +1,<br>f = 1 kHz, BW = 22 kHz | | 0,00032 | | % |
| | | $V_{IN}$ = 1 Vrms , $R_L$ = 1 kΩ, $A_V$ = +1,<br>f = 1 kHz, BW = 22 kHz | | 0,0004 | | |
| Φm | Phase margin | At unity gain, 25 °C, 10 kΩ, 100 pF | | 34 | | ° |
| $C_{LOAD}$ | Capacitive load drive | | | 100[4] | | pF |
| en | Input voltage noise density | f = 10 Hz | | 20 | | nV / √Hz |
| | | f = 100 Hz | | 13 | | |
| | | f = 10 kHz | | 12 | | |
| en p-p | Input noise voltage | 0.1 Hz ≤ f ≤ 10 Hz | | 0.8 | | $µV_{PP}$ |
| in | Input current noise density | f = 1 kHz | | 0.15 [5] | | pA / √Hz |

1. *See Section 5.4 Input offset voltage drift over the temperature in application information.*
2. *Current is positive when it is sinked into the op-amp.*
3. *$I_{io}$ is defined as $|I_{ibp} – I_{ibn}|$.*

4. *For higher capacitive values see Figure 24. Phase margin vs. output current at $V_{CC}$ = 5 V, Figure 26. Phase margin vs. capacitive load*
5. *Theoretical value of the input current noise density based on the measurement of the input transistor base current:* $i_n = \sqrt{2.q.i_b}$

# 4 Typical performance characteristics

$R_L$ connected to $V_{CC}$ / 2 (unless otherwise specified).

**Figure 3. Supply current vs. supply voltage**

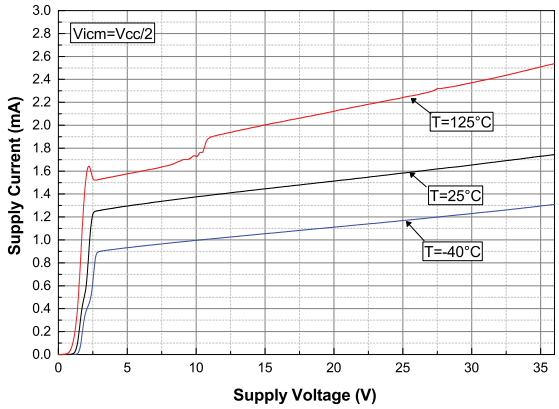


**Figure 4. Input offset voltage distribution at $V_{CC}$ = 5 V TSB712A**

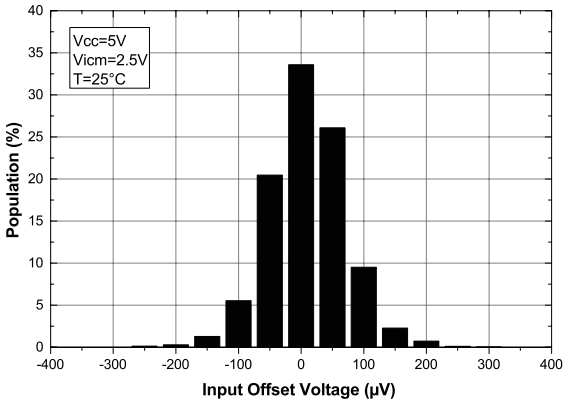


**Figure 5. Input offset voltage distribution at $V_{CC}$ = 36 V TSB712A**

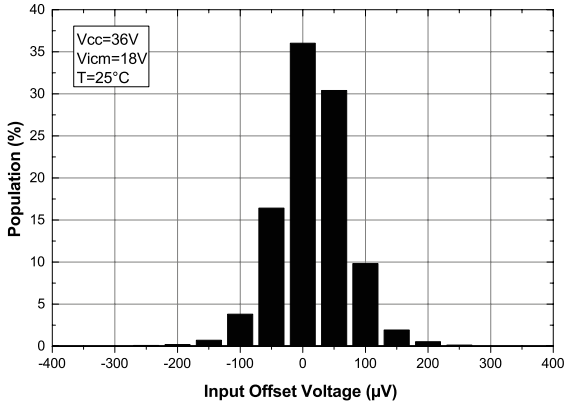


**Figure 6. Input offset voltage vs. temperature at $V_{CC}$ = 5 V**

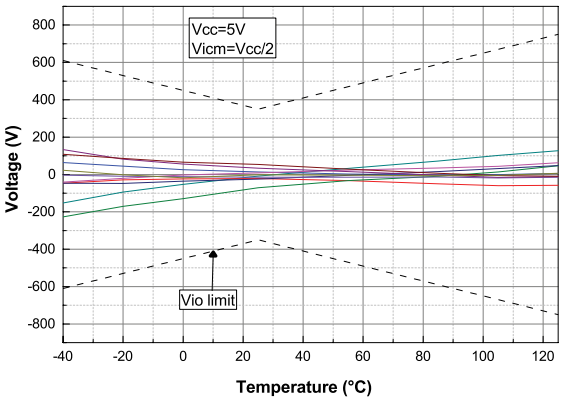

**Figure 7. Input offset voltage vs. temperature at $V_{CC}$ = 36 V**

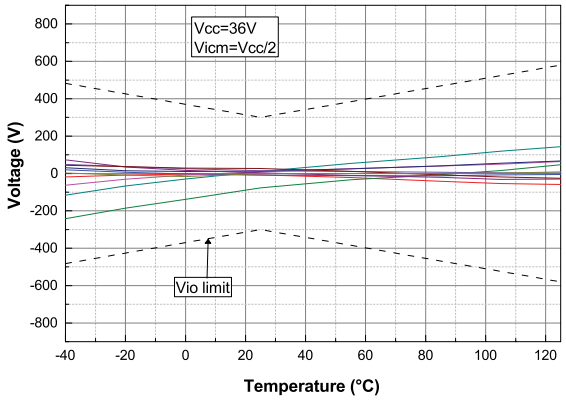


**Figure 8. Input offset voltage thermal coefficient distribution at $V_{CC}$ = 5 V**

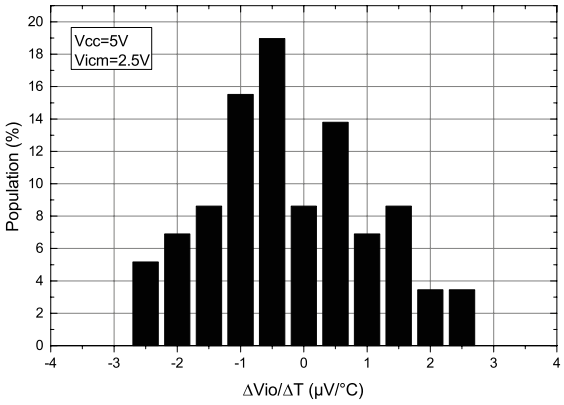


**Figure 9. Channel separation vs. frequency at $V_{CC}$ = 36 V**

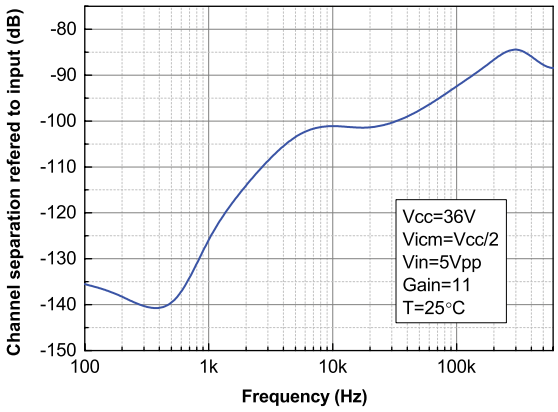


**Figure 10. Input offset voltage vs. supply voltage**

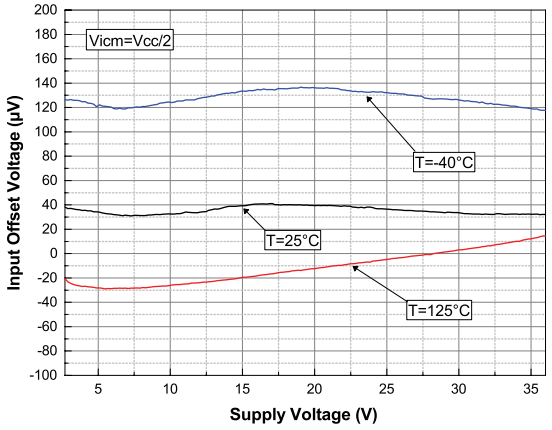


**Figure 11. Input offset voltage vs. common mode voltage at $V_{CC}$ = 5 V TSB712A**

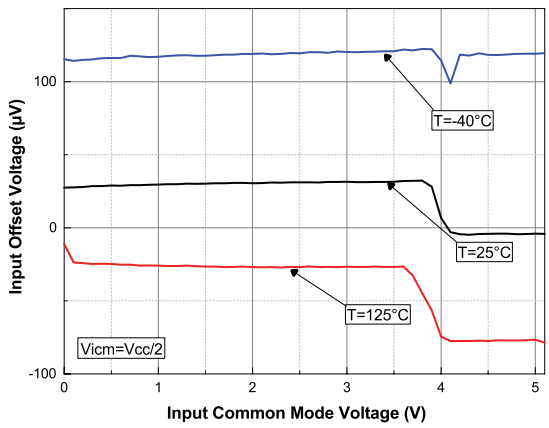


**Figure 12. Input offset voltage vs. common mode voltage at $V_{CC}$ = 36 V TSB712A**

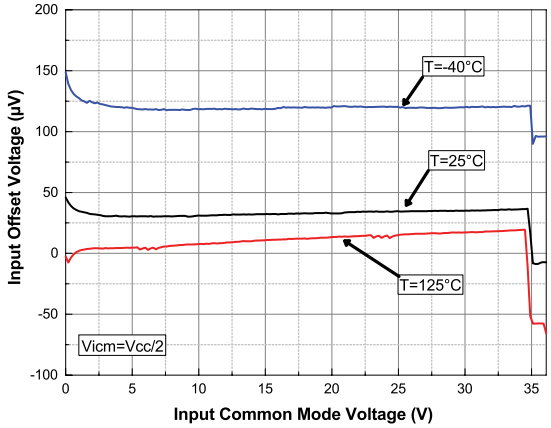

**Figure 13. Input bias current vs. temperature at $V_{ICM} = V_{CC} / 2$**

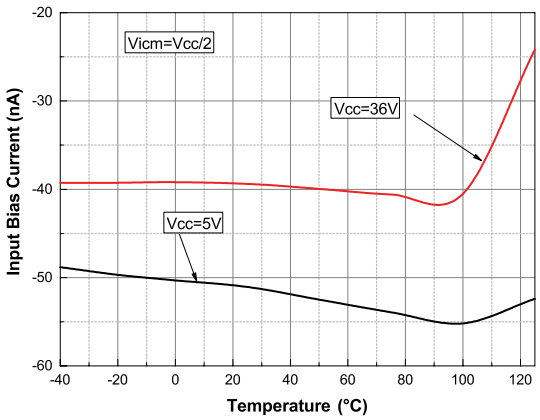


**Figure 14. Output current vs. output voltage at $V_{CC} = 5$ V**

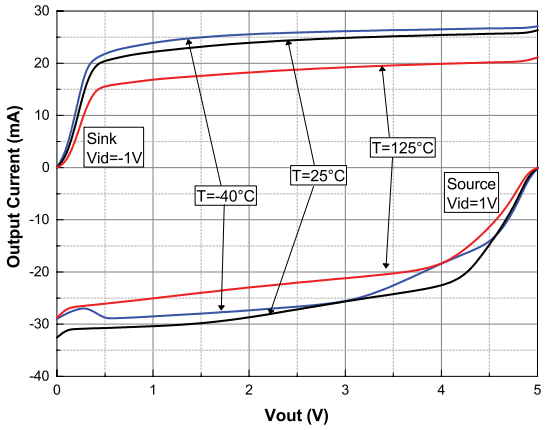


**Figure 15. Input bias current vs. common mode voltage at $V_{CC} = 5$ V**

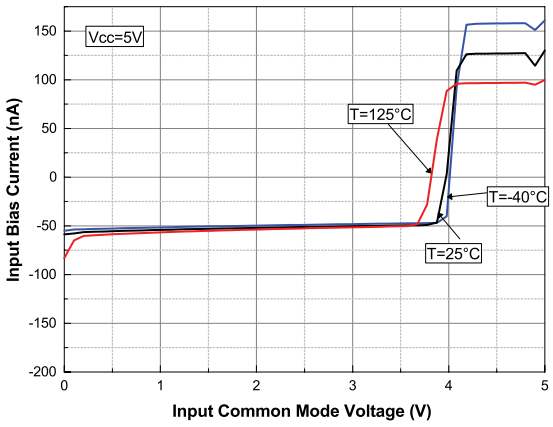


**Figure 16. Input bias current vs. common mode voltage at $V_{CC} = 36$ V**

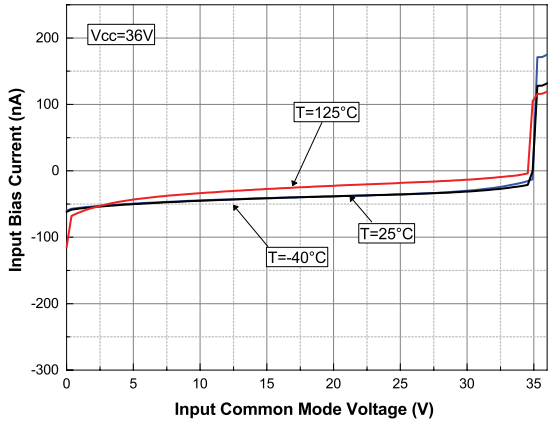


**Figure 17. Output current vs. output voltage at $V_{CC} = 36$ V**

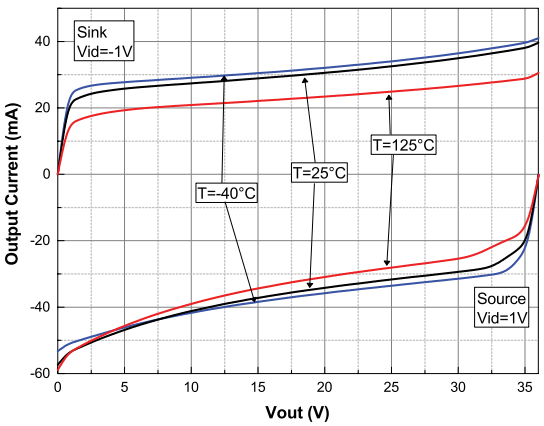


**Figure 18. Output voltage ($V_{OH}$) vs. supply voltage**

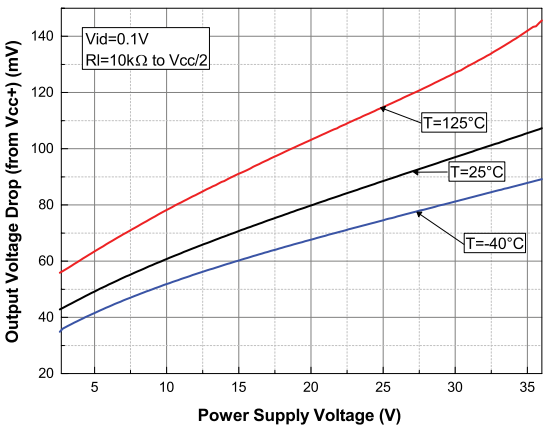

**Figure 19. Output voltage ($V_{OL}$) vs. supply voltage**

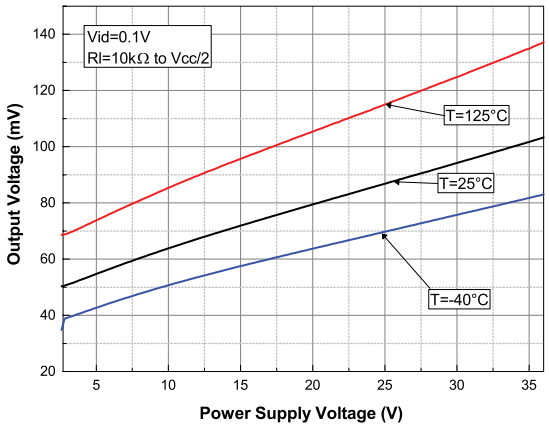


**Figure 20. Positive slew rate at $V_{CC}$ = 36 V**

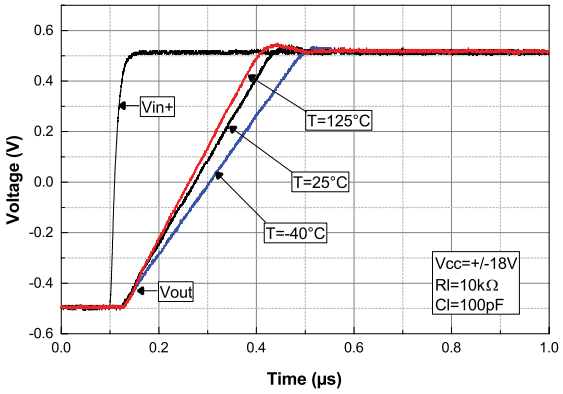


**Figure 21. Negative slew rate at $V_{CC}$ = 36 V**

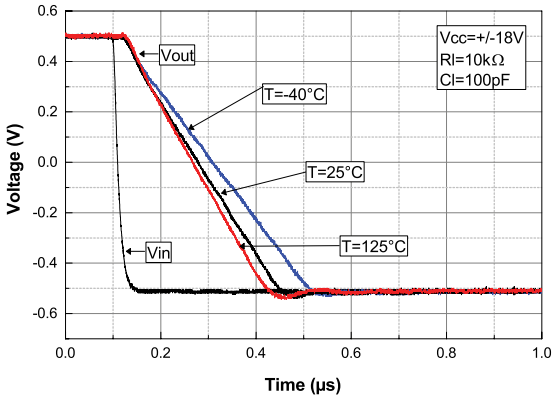


**Figure 22. Bode diagram at $V_{CC}$ = 5 V**

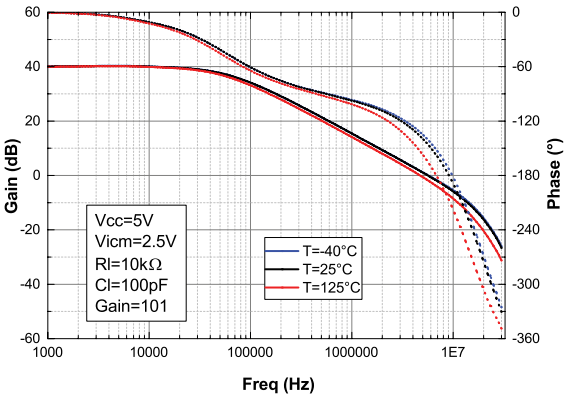


**Figure 23. Bode diagram at $V_{CC}$ = 36 V**

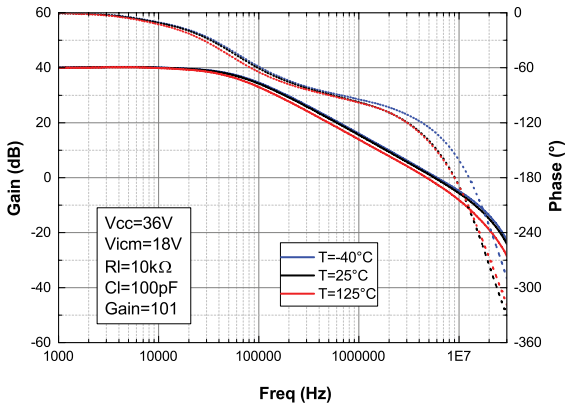


**Figure 24. Phase margin vs. output current at $V_{CC}$ = 5 V**

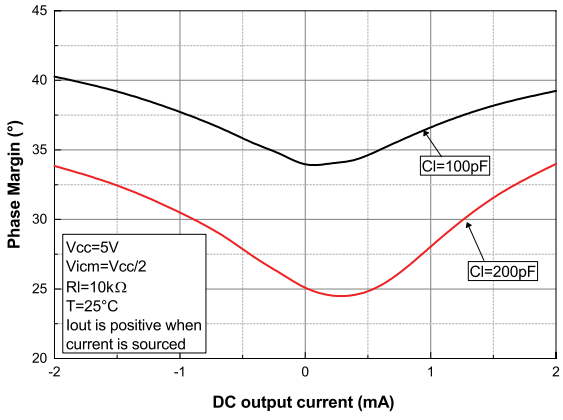

**Figure 25. Phase margin vs. output current at $V_{CC}$ = 36 V**

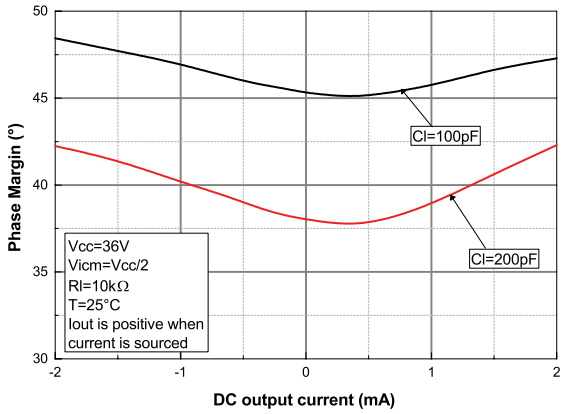


**Figure 26. Phase margin vs. capacitive load**

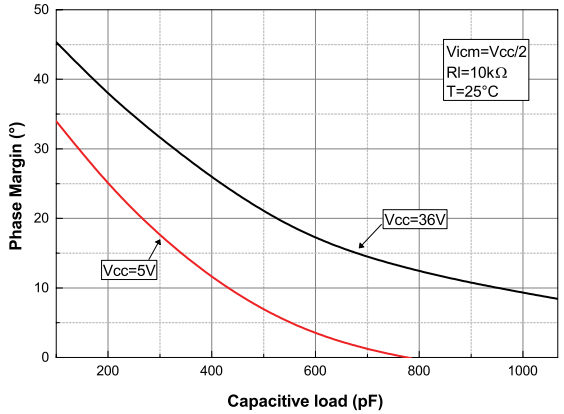


**Figure 27. Overshoot vs. capacitive load at $V_{CC}$ = 36 V**

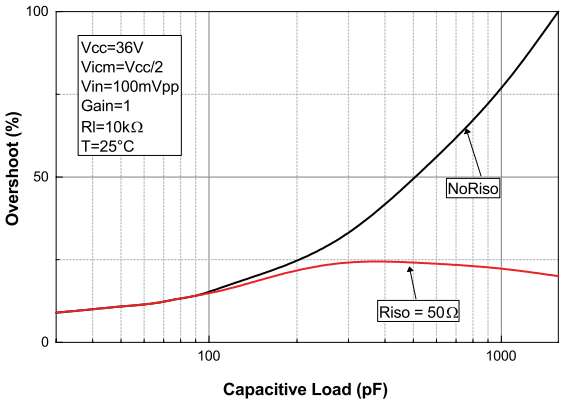


**Figure 28. Small step response vs. time at $V_{CC}$ = 5 V**

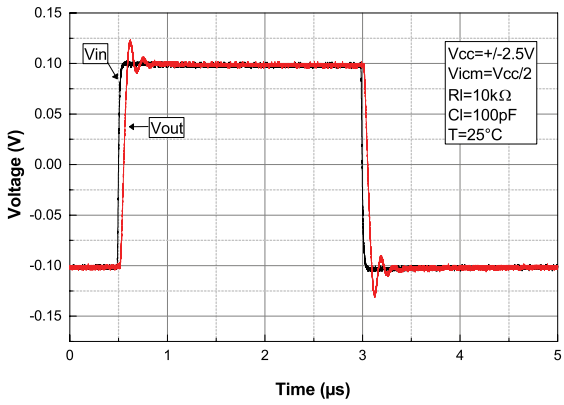


**Figure 29. Desaturation time at low rail at $V_{CC}$ = 5 V**

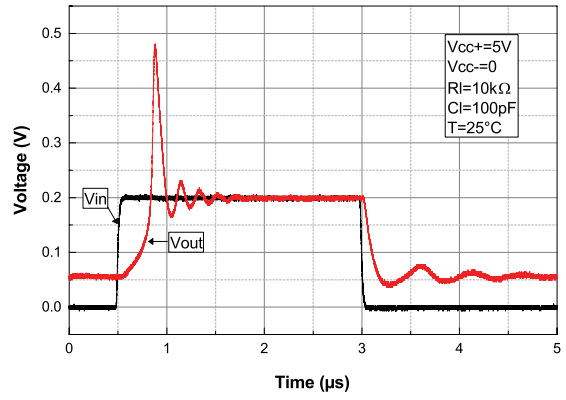


**Figure 30. Desaturation time at high rail at $V_{CC}$ = 5 V**

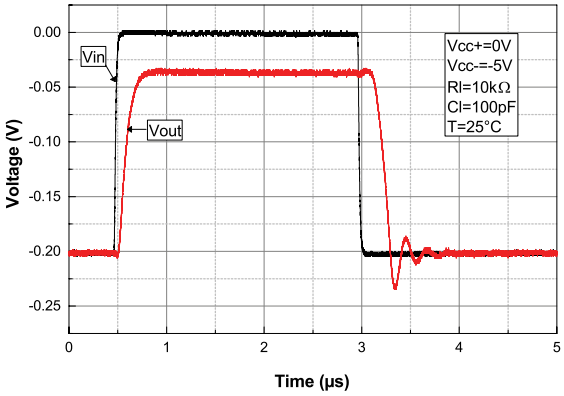

**Figure 31. Small step response vs. time at $V_{CC}$ = 36 V**

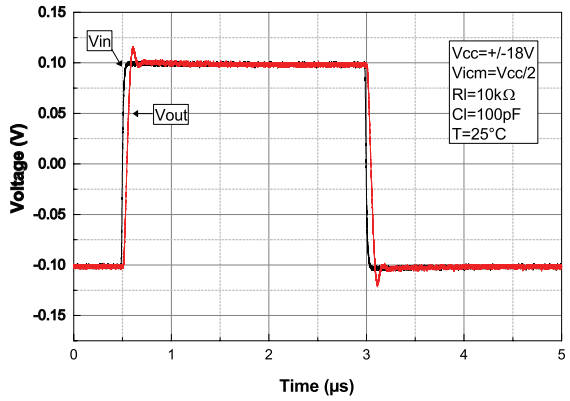


**Figure 32. Amplifier behavior close to the low rail at $V_{CC}$ = 36 V**

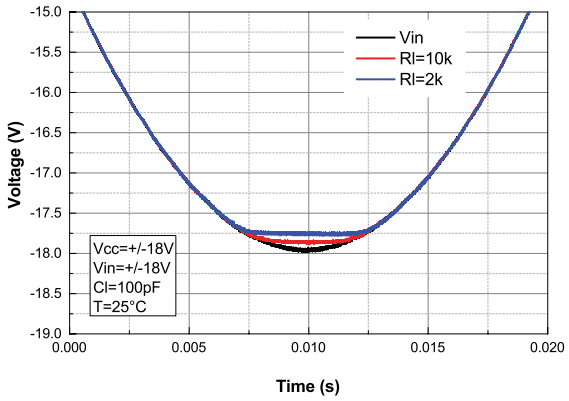


**Figure 33. Amplifier behavior close to the high rail at $V_{CC}$ = 36 V**

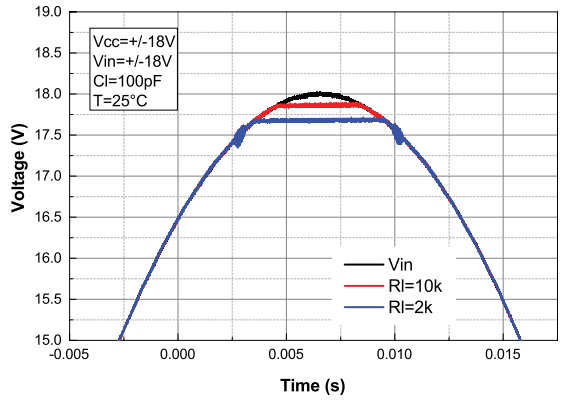


**Figure 34. Noise vs. frequency at $V_{CC}$ = 5 V**

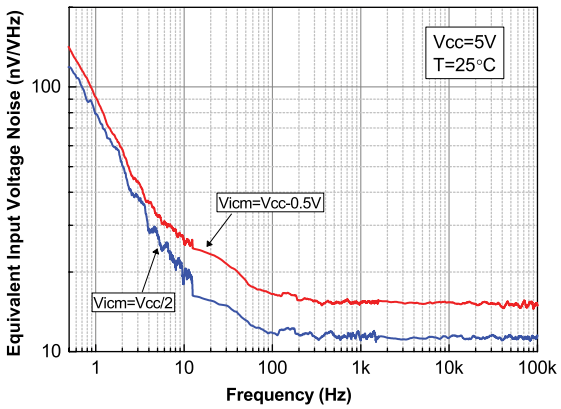


**Figure 35. Noise vs. frequency at $V_{CC}$ = 36 V**

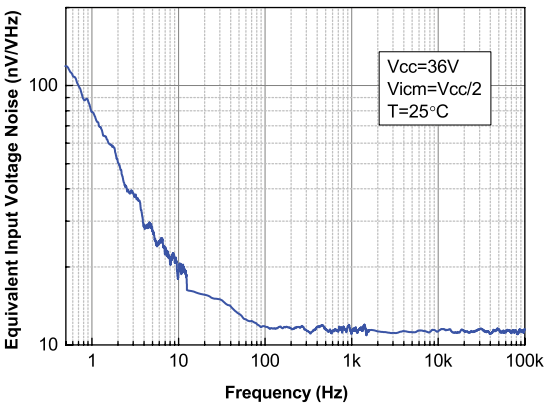


**Figure 36. Noise vs. time at $V_{CC}$ = 36 V**

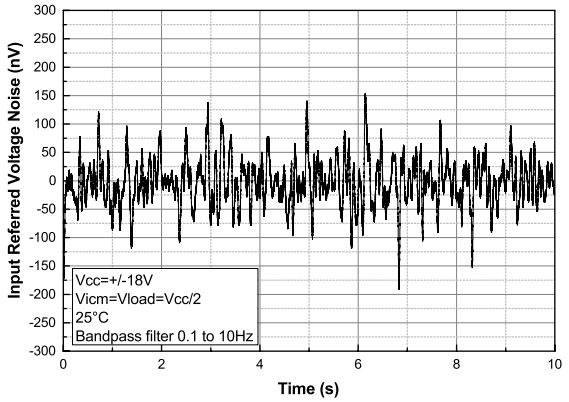

Figure 37. **THD+N vs. frequency**

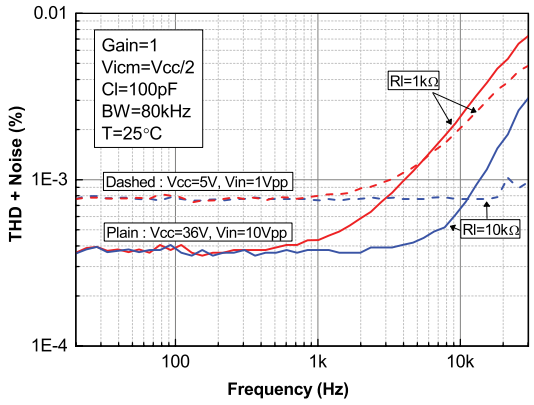


Figure 38. **THD+N vs. output voltage**

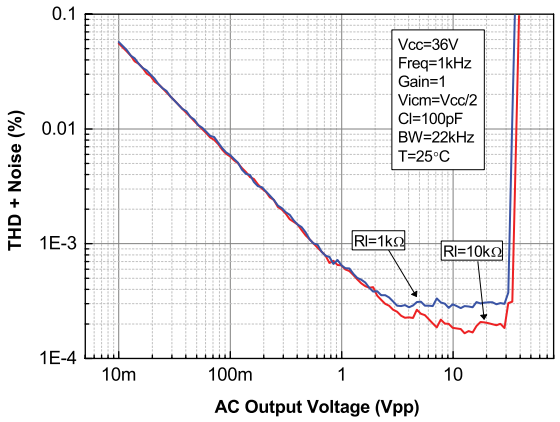


Figure 39. **PSRR vs. frequency at $V_{CC}$ = 10 V**

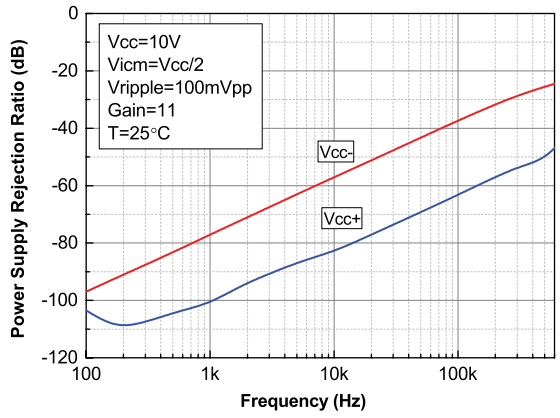


Figure 40. **CMRR vs. frequency at $V_{CC}$ = 10 V**

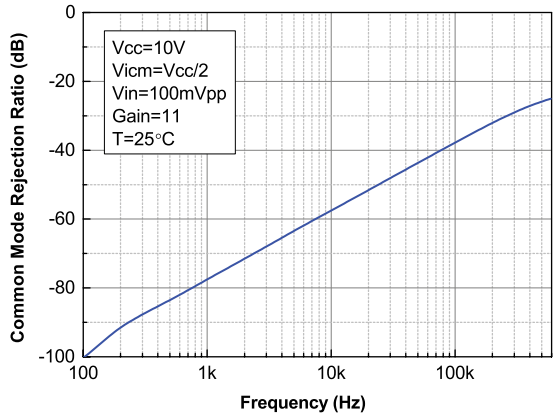

# 5 Application information

## 5.1 Operating voltages

The TSB712A/TSB712 devices can operate from 2.7 to 36 V. The parameters are fully specified at 5 V and 36 V power supplies. However, the parameters are very stable over the full $V_{CC}$ range and several characterization curves show the TSB712A/TSB712 device characteristics over the full operating range. Additionally, the main specifications are guaranteed in extended temperature range from -40 to 125 °C.

## 5.2 Input pin voltage range

The TSB712A/TSB712 devices have an internal ESD diode protection on the inputs. These diodes are connected between the inputs and each supply rail to protect the input stage from electrical discharge, as shown in the figure below.

**Figure 41. Input current limitation**

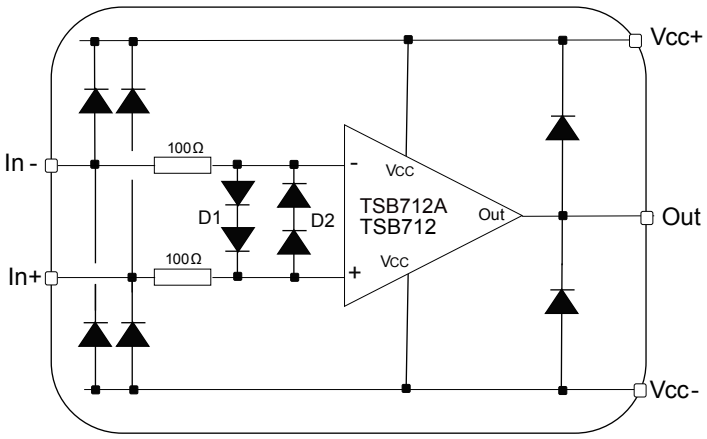


When the input pin voltage exceeds the power supply, the ESD diodes become conductive and, depending on this voltage, excessive current can flow through them. Without limitation this overcurrent can damage the device. In this case, the current has to be limited to 10 mA by adding a resistance in series with the input pin.

Similarly, in order to avoid excessive current in the protection diodes between the positive and negative inputs, the differential voltage should be limited to ± 2 V, or the current limited to 10 mA. Such a high differential voltage can be reached when the output is in saturation mode, or slew rate limited. In particular, it can happen when the device is used in comparator mode.

The TSB712A/TSB712 do not show any phase reversal for any input common mode voltage inside the absolute maximum ratings (AMR) voltage window, ($V_{CC-}$) - 200 mV < $V_{ICM}$ < ($V_{CC+}$) + 200 mV.

## 5.3 Rail-to-rail input stage

The TSB712A/TSB712 devices are built with two complementary NPN and PNP input differential pairs, as shown in the figure below.

**Figure 42. Rail-to-rail input stage**

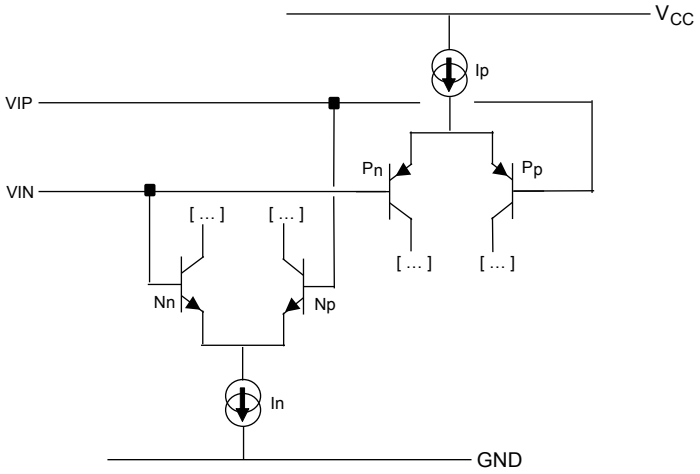


The devices have rail-to-rail inputs, and the input common mode range is extended from $V_{CC-}$ to ($V_{CC+}$) + 0.1 V. However, the performance of these devices is optimized for the P-channel differential pair (which means from $V_{CC-}$ to ($V_{CC+}$) - 1.5 V). Around ($V_{CC+}$) – 1 V, and with slight variations depending on the process, a transition occurs between the P-channel and the N-channel differential pair, impacting the input offset voltage (see Figure 11. Input offset voltage vs. common mode voltage at $V_{CC}$ = 5 V TSB712A and Figure 12. Input offset voltage vs. common mode voltage at $V_{CC}$ = 36 V TSB712A). As a consequence, CMRR can be degraded around this transition region. In order to achieve the best possible performance, this operating point should be avoided.

Please also notice that the input bias current polarity depends on the operation of NPN or PNP input stage. This transition is visible in figures Figure 15. Input bias current vs. common mode voltage at $V_{CC}$ = 5 V and Figure 16. Input bias current vs. common mode voltage at $V_{CC}$ = 36 V.

## 5.4 Input offset voltage drift over the temperature

The maximum input voltage drift variation over temperature is defined as the offset variation related to the offset value measured at 25 °C. The operational amplifier is one of the main circuits of the signal conditioning chain, and the amplifier input offset is a major contributor to the chain accuracy. The signal chain accuracy at 25 °C can be compensated during the production at application level. The maximum input voltage drift overtemperature enables the system designer to anticipate the effect of temperature variations. The maximum input voltage drift overtemperature is computed using the following formula:

$$\frac{\Delta V_{io}}{\Delta T} = \max\left|\frac{V_{io}(T) - V_{io}(25°C)}{T - 25°C}\right|_{T = -40\,°C \text{ and } T = 125\,°C} \quad (1)$$

The datasheet maximum value is guaranteed by a measurement on a representative sample size ensuring a Cpk (process capability index) greater than 1.3.

## 5.5 Long term input offset voltage drift

To evaluate product reliability, two types of stress acceleration are used:

- Voltage acceleration, by changing the applied voltage.
- Temperature acceleration, by changing the die temperature (below the maximum junction temperature allowed by the technology) with the ambient temperature.

The voltage acceleration has been defined based on JEDEC results, and is defined using:

(2)

$A_{FV} = e^{\beta.(V_S - V_U)}$

Where:

$A_{FV}$ is the voltage acceleration factor

β is the voltage acceleration coefficient in 1/V, constant technology parameter (β = 1)

$V_S$ is the stress voltage used for the accelerated test

$V_U$ is the voltage used for the application

The temperature acceleration is driven by the Arrhenius model, and is defined as follows:

(3)

$$A_{FT} = e^{\frac{E_a}{k} \cdot \left(\frac{1}{T_U} - \frac{1}{T_S}\right)}.$$

Where:

$A_{FT}$ is the temperature acceleration factor

$E_a$ is the activation energy of the technology based on the failure rate

k is the Boltzmann constant (8.6173 x $10^{-5}$ eV.$K^{-1}$)

$T_U$ is the temperature of the die when $V_U$ is used (K)

$T_S$ is the temperature of the die under temperature stress (K)

The final acceleration factor, $A_F$, is the multiplication of the voltage acceleration factor and the temperature acceleration factor.

(4)

$A_F = A_{FT} . A_{FV}$

$A_F$ is calculated using the temperature and voltage defined in the mission profile of the product. The $A_F$ value can then be used in Equation 5 to calculate the number of months of use equivalent to 1000 hours of reliable stress duration.

(5)

*Months = $A_F$ × 1000 h × 12 months / (24 h × 365.25 days)*

To evaluate the op-amp reliability, a follower stress condition is used where $V_{CC}$ is defined as a function of the maximum operating voltage and the absolute maximum ratings (as recommended by JEDEC rules). $V_{io}$ drift (in µV) of the product after 1000 h of stress is tracked with parameters at different measurement conditions.

(6)

$V_{CC} = max(V_{OP})$ *with* $V_{icm} = V_{CC}/2$

The long term drift parameter $\Delta V_{io}$ (in µV.$month^{-1/2}$), estimating the reliability performance of the product, is obtained using the ratio of the $V_{io}$ (input offset voltage value) drift over the square root of the calculated number of months.

(7)

$$\Delta V_{io} = \frac{V_{io}drift}{\sqrt{months}}$$

Where $V_{io}$ drift is the measured drift value in the specified test conditions after 1000 h stress duration.

The Vio final drift, in µV, to be measured on the device in real operation conditions can be computed from:

(8)

$$V_{io\ final\ drift}(t_{op}, T_{op}, V_{CC}) = \Delta V_{io,\ 25°C} \cdot \sqrt{t_{op} \cdot e^{\beta \cdot (V_{CC} - V_{CC\ nom})} \cdot e^{\frac{E_a}{k} \cdot \left(\frac{1}{297} - \frac{1}{T_{op}}\right)}}$$

Where:

$\Delta V_{io}$ is the long term drift parameter in µV.month$^{-1/2}$

$t_{op}$ is the operating time seen by the device, in months

$T_{op}$ is the operating temperature

$V_{CC}$ is the power supply during operating time

$V_{CC}$ nom is the nominal $V_{CC}$ at which the $\Delta V_{io}$ is computed (36 V for the TSB712A).

$E_a$ is the activation energy of the technology (here 0.7 eV).

## 5.6 EMI rejection

The electromagnetic interference (EMI) rejection ratio, or EMIRR, describes the EMI immunity of operational amplifiers. An adverse effect that is common to many op-amps is a change in the offset voltage as a result of RF signal rectification. EMIRR is defined as follows:

$$EMIRR = 20.\log\left(\frac{V_{in\,pp}}{\Delta V_{io}}\right) \quad (9)$$

The TSB712A/TSB712 have been specially designed to minimize susceptibility to EMIRR and shows a low sensitivity. As visible on figure below, EMI rejection ratio has been measured on both inputs and outputs, from 400 MHz to 2.4 GHz.

**Figure 43. EMIRR on In+, In- and out pins**

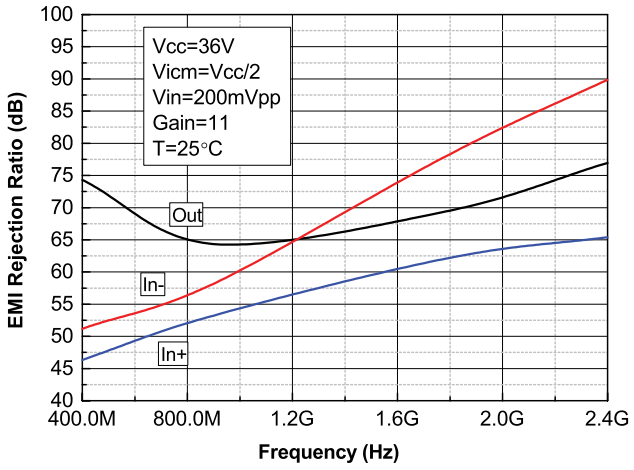


EMIRR performance might be improved by adding small capacitances (in the pF range) on the inputs, power supply and output pins. These capacitances help in minimizing the impedance of these nodes at high frequencies.

## 5.7 Maximum power dissipation

The usable output load current drive is limited by the maximum power dissipation allowed by the device package. The absolute maximum junction temperature for the TSB712A is 150 °C. The junction temperature can be estimated as follows:

$$T_J = P_D \times R_{th-ja} + T_A \quad (10)$$

$T_J$ is the die junction temperature

$P_D$ is the power dissipated in the package

$R_{th\text{-}ja}$ is the junction to ambient thermal resistance of the package

$T_A$ is the ambient temperature

The power dissipated in the package $P_D$ is the sum of the quiescent power dissipated and the power dissipated by the output stage transistor. It is calculated as follows:

$$P_D = (V_{CC} \times I_{CC}) + (V_{CC+} - V_{OUT}) \times ILoad \quad (11)$$

when the op-amp sources the current

$$P_D = (V_{CC} \times I_{CC}) + (V_{OUT} - V_{CC-}) \times ILoad \quad (12)$$

when the op-amp is sinks the current.

Do not exceed the 150 °C maximum junction temperature for the device. Exceeding the junction temperature limit can cause degradation in the parametric performance or even destroy the device.

## 5.8 Capacitive load and stability

Stability analysis must be performed for large capacitive loads over 100 pF. Increasing the load capacitance to high values produces gain peaking in the frequency response, with overshoot and ringing in the step response.

Generally, unity gain configuration is the worst situation for stability and the ability to drive large capacitive loads. For additional capacitive load drive capability in unity-gain configuration, stability can be improved by inserting a small resistor $R_{ISO}$ (10 Ω to 30 Ω) in series with the output. This resistor significantly reduces ringing while maintaining DC performance for purely capacitive loads. However, if there is a resistive load in parallel with the capacitive load, a voltage divider is created introducing a gain error on the output and slightly reducing the output swing. The error introduced is proportional to the ratio $R_{ISO}$ / $R_L$. $R_{ISO}$ modifies the maximum capacitive load acceptable from a stability point-of-view as described in the following figure:

**Figure 44. Stability criteria with a serial resistor at different capacitive loads**

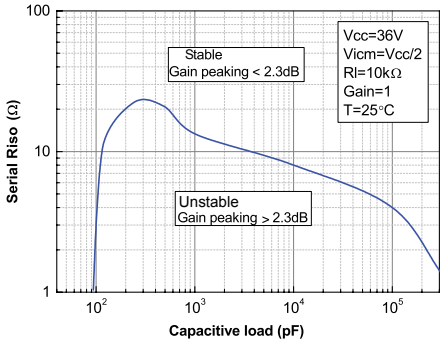

Figure 45. **Test configuration for $R_{ISO}$**

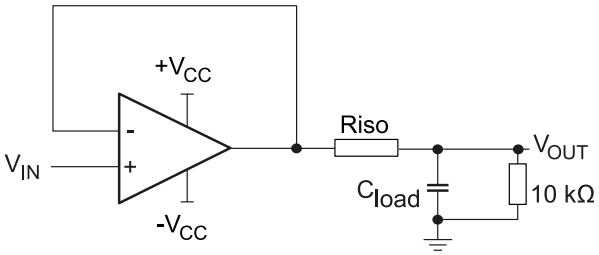


Please note that $R_{ISO}$ = 30 Ω is sufficient to make the TSB712A/TSB712 stable whatever the capacitive load.

## 5.9 PCB layout recommendations

Particular attention must be paid to the layout of the PCB tracks connected to the amplifier, load, and power supply. The power and ground traces are critical as they must provide adequate energy and grounding for all circuits. The best practice is to use short and wide PCB traces to minimize voltage drops and parasitic inductance. In addition, to minimize parasitic impedance over the entire surface, a multi-via technique that connects the bottom and top layer ground planes together in many locations is often used. The copper traces connecting the output pins to the load and supply pins should be as wide as possible to minimize trace resistance.

## 5.10 Decoupling capacitor

In order to ensure op-amp full functionality, it is mandatory to place a decoupling capacitor of at least 22 nF as close as possible to the op-amp supply pin. A good decoupling helps to reduce electromagnetic interference impact.

# 6 Typical applications

## 6.1 Low-side current sensing

Power management mechanisms are found in most electronic systems. Current sensing is useful to protect applications. The low-side current sensing method consists of placing a sense resistor between the load and the circuit ground. The resulting voltage drop is amplified using the TSB712A (see the following figure).

**Figure 46. Low-side current sensing schematic**

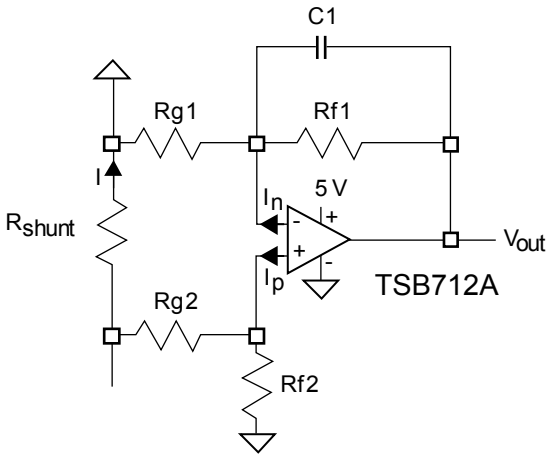


$V_{out}$ can be expressed as follows:

$$V_{OUT} = R_{shunt}.I\left(1 - \frac{R_{g2}}{R_{g2} + R_{f2}}\right).\left(1 - \frac{R_{f1}}{R_{g1}}\right) + I_p.\frac{R_{g2}.R_{f2}}{R_{g2} + R_{f2}}.\left(1 + \frac{R_{f1}}{R_{g1}}\right) - I_n.R_{f1} - V_{io}.\left(1 - \frac{R_{f1}}{R_{g1}}\right) \quad (13)$$

Assuming that $R_{f2} = R_{f1} = R_f$ and $R_{g2} = R_{g1} = R_g$, can be simplified in the following manner:

$$V_{OUT} = R_{shunt}.I.\frac{R_f}{R_g} - V_{io}.\left(1 + \frac{R_f}{R_g}\right) + R_f.I_{io} \quad (14)$$

The main advantage of using the TSB712A for a low-side current sensing relies on its low $V_{io}$, compared to general purpose operational amplifiers. For the same current and targeted accuracy, the shunt resistor can be chosen with a lower value, resulting in lower power dissipation, lower drop in the ground path, and lower cost. Particular attention must be paid to the matching and precision of $R_{g1}$, $R_{g2}$, $R_{f1}$, and $R_{f2}$, to maximize the accuracy of the measurement.

# 7 Package information

In order to meet environmental requirements, ST offers these devices in different grades of ECOPACK® packages, depending on their level of environmental compliance. ECOPACK® specifications, grade definitions and product status are available at: www.st.com. ECOPACK® is an ST trademark.

## 7.1 MiniSO8 package information

Figure 47. **MiniSO8 package outline**

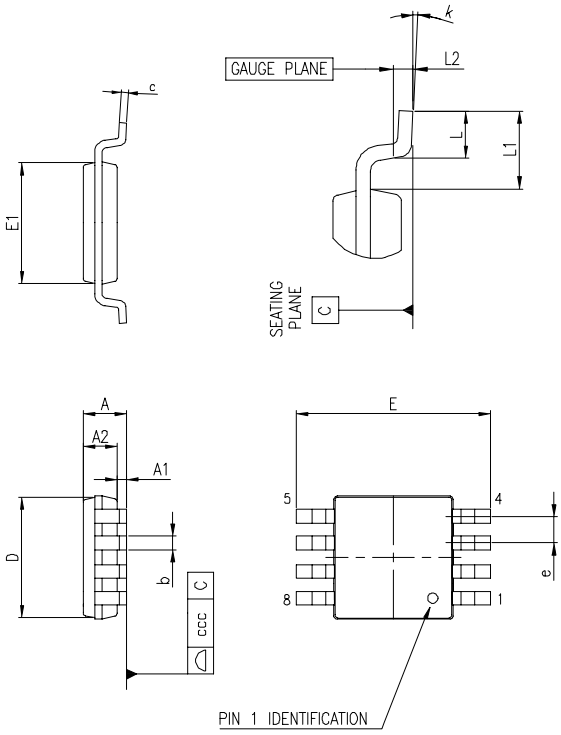


Table 5. **MiniSO8 mechanical data**

| Dim. | Millimeters | | | Inches | | |
|---|---|---|---|---|---|---|
| | Min. | Typ. | Max. | Min. | Typ. | Max. |
| A | | | 1.1 | | | 0.043 |
| A1 | 0 | | 0.15 | 0 | | 0.006 |
| A2 | 0.75 | 0.85 | 0.95 | 0.03 | 0.033 | 0.037 |
| b | 0.22 | | 0.4 | 0.009 | | 0.016 |
| c | 0.08 | | 0.23 | 0.003 | | 0.009 |
| D | 2.8 | 3 | 3.2 | 0.11 | 0.118 | 0.126 |
| E | 4.65 | 4.9 | 5.15 | 0.183 | 0.193 | 0.203 |
| E1 | 2.8 | 3 | 3.1 | 0.11 | 0.118 | 0.122 |
| e | | 0.65 | | | 0.026 | |
| L | 0.4 | 0.6 | 0.8 | 0.016 | 0.024 | 0.031 |
| L1 | | 0.95 | | | 0.037 | |
| L2 | | 0.25 | | | 0.01 | |
| k | 0° | | 8° | 0° | | 8° |
| ccc | | | 0.1 | | | 0.004 |

## 7.2 SO8 package information

Figure 48. **SO8 package outline**

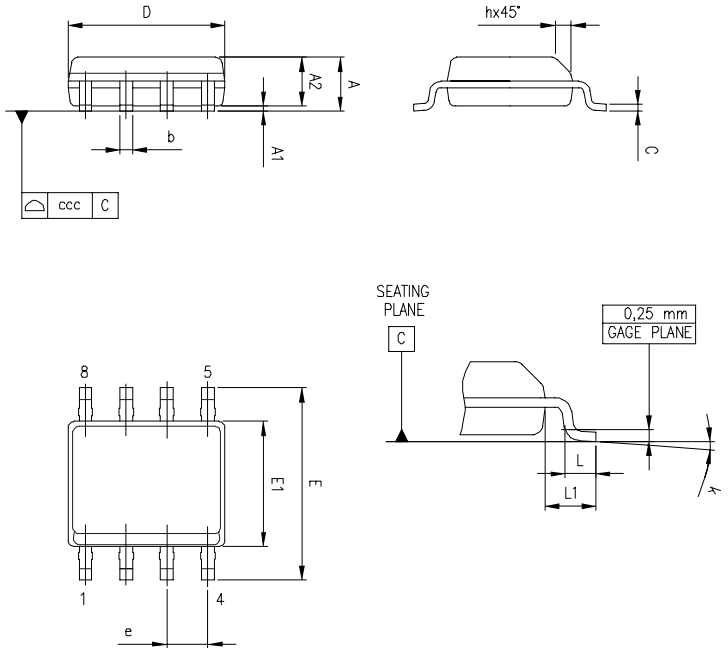


Table 6. **SO-8 mechanical data**

| Dim. | mm | | | Inches | | |
|---|---|---|---|---|---|---|
| | Min. | Typ. | Max. | Min. | Typ. | Max. |
| A | | | 1.75 | | | 0.069 |
| A1 | 0.1 | | 0.25 | 0.004 | | 0.01 |
| A2 | 1.25 | | | 0.049 | | |
| b | 0.28 | | 0.48 | 0.011 | | 0.019 |
| c | 0.17 | | 0.23 | 0.007 | | 0.01 |
| D | 4.8 | 4.9 | 5 | 0.189 | 0.193 | 0.197 |
| E | 5.8 | 6 | 6.2 | 0.228 | 0.236 | 0.244 |
| E1 | 3.8 | 3.9 | 4 | 0.15 | 0.154 | 0.157 |
| e | | 1.27 | | | 0.05 | |
| h | 0.25 | | 0.5 | 0.01 | | 0.02 |
| L | 0.4 | | 1.27 | 0.016 | | 0.05 |
| L1 | | 1.04 | | | 0.04 | |
| k | 0 | | 8 ° | 1 ° | | 8 ° |
| ccc | | | 0.1 | | | 0.004 |

# 8 Ordering information

Table 7. **Order code**

| Order code | Temperature range | Package | Packing | Marking |
|---|---|---|---|---|
| TSB712AIST | -40° to +125 °C | MiniSO8 | Tape and reel | K214 |
| TSB712AIDT | | SO8 | | TSB712AI |
| TSB712IDT | | SO8 | | TSB712I |
| TSB712IST | | MiniSO8 | | 712S |
| TSB712AIYDT | -40 to 125 °C automotive grade(1) | SO8 | | 712AIY |
| TSB712AIYST | | MiniSO8 | | 712Y |
| TSB712IYDT | | SO8 | | 712IY |
| TSB712IYST | | MiniSO8 | | K215 |

1. *Qualified and characterized according to AEC Q100 and Q003 or equivalent, advanced screening according to AEC Q001 and Q002 or equivalent.*

DFN8 package may be available for qualification under customer request. Please contact sales office for such request.

## Revision history

**Table 8. Document revision history**

| Date | Revision | Changes |
|---|---|---|
| 23-Apr-2018 | 1 | Initial release. |
| 17-Sep-2018 | 2 | Added the TSB712 as root part number; cover page has been updated accordingly.<br>Updated Section 3 Electrical characteristics, Section 4 Typical performance characteristics, Section 5 Application information and Table 7. Order code.<br>Added Section 7.2 SO8 package information. |
| 29-Nov-2018 | 3 | Updated Table 3. Electrical characteristics at $V_{CC}$ = 36 V, $V_{ICM}$ = $V_{OUT}$ = $V_{CC}$ / 2, $T_{amb}$ = 25 °C and $R_L$ connected to $V_{CC}$ / 2 (unless otherwise specified) and Table 4. Electrical characteristics at $V_{CC}$ = 5 V, $V_{ICM}$ = $V_{OUT}$ = $V_{CC}$ / 2, $T_{amb}$ = 25 °C and $R_L$ connected to $V_{CC}$ / 2 (unless otherwise specified). |
| 18-Feb-2019 | 4 | Updated Figure 44. Stability criteria with a serial resistor at different capacitive loads |

# Contents

1 **Pin description** . . . . . 2
2 **Absolute maximum ratings and operating conditions** . . . . . 3
3 **Electrical characteristics** . . . . . 4
4 **Typical performance characteristics** . . . . . 10
5 **Application information** . . . . . 17
5.1 Operating voltages . . . . . 17
5.2 Input pin voltage range . . . . . 17
5.3 Rail-to-rail input stage . . . . . 18
5.4 Input offset voltage drift over the temperature . . . . . 18
5.5 Long term input offset voltage drift . . . . . 19
5.6 EMI rejection . . . . . 20
5.7 Maximum power dissipation . . . . . 21
5.8 Capacitive load and stability . . . . . 21
5.9 PCB layout recommendations . . . . . 23
5.10 Decoupling capacitor . . . . . 23
6 **Typical applications** . . . . . 24
6.1 Low-side current sensing . . . . . 24
7 **Package information** . . . . . 25
7.1 MiniSO8 package information . . . . . 26
7.2 SO8 package information . . . . . 26
8 **Ordering information** . . . . . 28
**Revision history** . . . . . 29

# List of tables

Table 1. Absolute maximum ratings . . . 3
Table 2. Operating conditions . . . 3
Table 3. Electrical characteristics at $V_{CC}$ = 36 V, $V_{ICM}$ = $V_{OUT}$ = $V_{CC}$ / 2, $T_{amb}$ = 25 °C and $R_L$ connected to $V_{CC}$ / 2 (unless otherwise specified) . . . 4
Table 4. Electrical characteristics at $V_{CC}$ = 5 V, $V_{ICM}$ = $V_{OUT}$ = $V_{CC}$ / 2, $T_{amb}$ = 25 °C and $R_L$ connected to $V_{CC}$ / 2 (unless otherwise specified) . . . 7
Table 5. MiniSO8 mechanical data . . . 26
Table 6. SO-8 mechanical data . . . 27
Table 7. Order code . . . 28
Table 8. Document revision history . . . 29

# List of figures

Figure 2. Pin connections (top view) . . . 2
Figure 3. Supply current vs. supply voltage . . . 10
Figure 4. Input offset voltage distribution at $V_{CC}$ = 5 V TSB712A . . . 10
Figure 5. Input offset voltage distribution at $V_{CC}$ = 36 V TSB712A . . . 10
Figure 6. Input offset voltage vs. temperature at $V_{CC}$ = 5 V . . . 10
Figure 7. Input offset voltage vs. temperature at $V_{CC}$ = 36 V . . . 11
Figure 8. Input offset voltage thermal coefficient distribution at $V_{CC}$ = 5 V . . . 11
Figure 9. Channel separation vs. frequency at $V_{CC}$ = 36 V . . . 11
Figure 10. Input offset voltage vs. supply voltage . . . 11
Figure 11. Input offset voltage vs. common mode voltage at $V_{CC}$ = 5 V TSB712A . . . 11
Figure 12. Input offset voltage vs. common mode voltage at $V_{CC}$ = 36 V TSB712A . . . 11
Figure 13. Input bias current vs. temperature at $V_{ICM} = V_{CC} / 2$ . . . 12
Figure 14. Output current vs. output voltage at $V_{CC}$ = 5 V . . . 12
Figure 15. Input bias current vs. common mode voltage at $V_{CC}$ = 5 V . . . 12
Figure 16. Input bias current vs. common mode voltage at $V_{CC}$ = 36 V . . . 12
Figure 17. Output current vs. output voltage at $V_{CC}$ = 36 V . . . 12
Figure 18. Output voltage ($V_{OH}$) vs. supply voltage . . . 12
Figure 19. Output voltage ($V_{OL}$) vs. supply voltage . . . 13
Figure 20. Positive slew rate at $V_{CC}$ = 36 V . . . 13
Figure 21. Negative slew rate at $V_{CC}$ = 36 V . . . 13
Figure 22. Bode diagram at $V_{CC}$ = 5 V . . . 13
Figure 23. Bode diagram at $V_{CC}$ = 36 V . . . 13
Figure 24. Phase margin vs. output current at $V_{CC}$ = 5 V . . . 13
Figure 25. Phase margin vs. output current at $V_{CC}$ = 36 V . . . 14
Figure 26. Phase margin vs. capacitive load . . . 14
Figure 27. Overshoot vs. capacitive load at $V_{CC}$ = 36 V . . . 14
Figure 28. Small step response vs. time at $V_{CC}$ = 5 V . . . 14
Figure 29. Desaturation time at low rail at $V_{CC}$ = 5 V . . . 14
Figure 30. Desaturation time at high rail at $V_{CC}$ = 5 V . . . 14
Figure 31. Small step response vs. time at $V_{CC}$ = 36 V . . . 15
Figure 32. Amplifier behavior close to the low rail at $V_{CC}$ = 36 V . . . 15
Figure 33. Amplifier behavior close to the high rail at $V_{CC}$ = 36 V . . . 15
Figure 34. Noise vs. frequency at $V_{CC}$ = 5 V . . . 15
Figure 35. Noise vs. frequency at $V_{CC}$ = 36 V . . . 15
Figure 36. Noise vs. time at $V_{CC}$ = 36 V . . . 15
Figure 37. THD+N vs. frequency . . . 16
Figure 38. THD+N vs. output voltage . . . 16
Figure 39. PSRR vs. frequency at $V_{CC}$ = 10 V . . . 16
Figure 40. CMRR vs. frequency at $V_{CC}$ = 10 V . . . 16
Figure 41. Input current limitation . . . 17
Figure 42. Rail-to-rail input stage . . . 18
Figure 43. EMIRR on In+, In- and out pins . . . 20
Figure 44. Stability criteria with a serial resistor at different capacitive loads . . . 21
Figure 45. Test configuration for $R_{ISO}$ . . . 22
Figure 46. Low-side current sensing schematic . . . 24
Figure 47. MiniSO8 package outline . . . 26
Figure 48. SO8 package outline . . . 27

**IMPORTANT NOTICE – PLEASE READ CAREFULLY**

STMicroelectronics NV and its subsidiaries (“ST”) reserve the right to make changes, corrections, enhancements, modifications, and improvements to ST products and/or to this document at any time without notice. Purchasers should obtain the latest relevant information on ST products before placing orders. ST products are sold pursuant to ST’s terms and conditions of sale in place at the time of order acknowledgement.

Purchasers are solely responsible for the choice, selection, and use of ST products and ST assumes no liability for application assistance or the design of Purchasers’ products.

No license, express or implied, to any intellectual property right is granted by ST herein.

Resale of ST products with provisions different from the information set forth herein shall void any warranty granted by ST for such product.

ST and the ST logo are trademarks of ST. All other product or service names are the property of their respective owners.

Information in this document supersedes and replaces information previously supplied in any prior versions of this document.

© 2019 STMicroelectronics – All rights reserved